

Short Communication

Metallic NiFe as Bifunctional Electrocatalysts for Efficient Urea Conversion

Mengwei Xue¹, Zhou Zhou¹, Jingwen Yu¹, Benzhi Liu², Shiyuan Qi¹, Qinpu Liu¹,
Guangqing Liu^{1,*}

¹ School of Environmental Science, Nanjing Xiaozhuang University, Nanjing, China, Postcode: 211171.

² School of Environmental Science and Engineering, Yancheng Institute of Technology, Yancheng, China, Postcode: 224051.

*E-mail: guangqingliu025@163.com

Received: 8 August 2020 / Accepted: 23 September 2020 / Published: 31 October 2020

A simple electrodeposition method was used to prepare metallic NiFe on nickel foam(NiFe/NF). NiFe/NF showed excellent electrocatalytic activities for HER and UOR in an alkaline solution containing urea. The electrochemically active surface area(ESCA) measurements indicating that NiFe/NF has an improved ESCA and more active sites. Metallic NiFe can be used as a bifunctional catalyst for efficient urea oxidation and electrocatalytic hydrogen evolution.

Keywords: Electrodeposition; Electrocatalytic oxidation; Urea

1. INTRODUCTION

Electrochemical water splitting has a broad prospect in alleviating the global energy crisis [1,2]. Hydrogen produced by water splitting is an alternative to fossil energy[3-6]. Oxygen evolution reaction (OER), as an important water splitting half-reaction, requires a high overpotential, which seriously hinders the efficiency of water splitting[7]. To solve this problem, many efforts have been made to develop highly active catalysts[8]. Some progress has been made, such as increasing the number of active sites and enhancing the electrocatalytic activity[9-12]. However, the overpotential is still higher than 0.2 V[13].

Urea oxidation reaction (UOR) is expected to be an anode reaction instead of OER. This is due to the low decomposition potential (0.37 V) of UOR, cheap raw materials, a wide range of sources, and nontoxic N₂ and CO₂ produced during electrochemical reactions[14-17]. Therefore, it is necessary to develop UOR to replace OER. Electrocatalytic UOR usually takes place through the following reaction

paths: $\text{CO}(\text{NH}_2)_2 + \text{H}_2\text{O} \rightarrow \text{N}_2 + 3\text{H}_2 + \text{CO}_2$.

There are many substances, such as alloys [18], oxides [19, 20], phosphides, and hydroxides [21, 22] have been studied as UOR catalysts. In these electrocatalysts, transition metal Ni and their alloys have excellent UOR activity [23]. The structure and morphology of nickel play an important role in the catalytic performance of the material. Increasing the specific surface area of the catalyst by producing zero- and one-dimensional nickel could enlarge the reaction site and achieve a higher electrochemical active area [24, 25]. Botte et al. [26] used other metals (Mn, Co, Mo, Zn, Fe) and Ni alloys as electrocatalysts to improve the electrocatalytic activity of urea oxidation. Because the synthesis methods of alloy materials are diverse and simple, different metal doping is used to produce more active sites to reduce the electrocatalytic reaction potential.

In this work, a simple electrodeposition method was used to synthesize metallic NiFe on nickel foam, which reduced complexity of synthetic process. In alkaline solution, metallic NiFe shows excellent UOR activity, at the same time, it also shows excellent hydrogen evolution reaction (HER) catalytic property. Moreover, metallic NiFe is much cheaper than other precious metals. Therefore, Metallic NiFe can be used as a promising bifunctional catalyst for efficient urea oxidation and electrocatalytic hydrogen evolution.

2. EXPERIMENTAL

2.1. Reagents and instrumentation

Ferrous sulfate heptahydrate ($\text{FeSO}_4 \cdot 7\text{H}_2\text{O}$), nickel sulfate hexahydrate ($\text{NiSO}_4 \cdot 6\text{H}_2\text{O}$), Urea (H_2NCONH_2) and potassium hydroxide (KOH) were purchased from China Pharmaceutical Group Chemical Reagents Co., Ltd.

All the electrochemical experiments were performed on a CHI660B electrochemical workstation (Chenhua Instrument Company of Shanghai, China) with a conventional three-electrode system.

2.2. Preparation of Ni/NF and NiFe/NF

The Ni/NF and NiFe/NF electrodes were prepared through a one-step electrodeposition method. Before electrodeposition, the Ni foam (NF, $1 \text{ cm} \times 1 \text{ cm}$) was immersed in 3 M HCl solution for 10 min to remove the surface oxides, subsequently by sonication with ethanol and double-distilled water, then left to dry in air. The electrodeposition was performed in a three-electrode cell, NF as the working electrode, a saturated calomel electrode (SCE) as the reference electrode, and Pt as the counter electrode. For electrodeposition, the electrolytic solutions of 50 mM $\text{NiSO}_4 \cdot 6\text{H}_2\text{O}$ or 25 mM $\text{NiSO}_4 \cdot 6\text{H}_2\text{O}$ and 25 mM $\text{FeSO}_4 \cdot 7\text{H}_2\text{O}$ was used to prepare Ni/NF and NiFe/NF electrodes. Electrodeposition potential is -1V and electrodeposition time is 300s. After electrodeposition, the electrodes were carefully cleaned with double-distilled water and then dried in air.

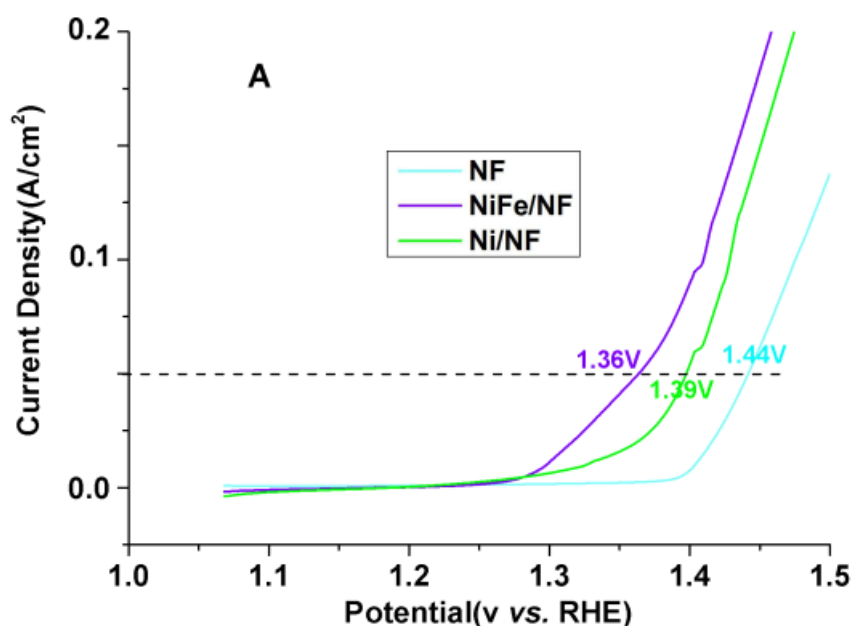
2.3. Electrochemical measurements

Electrochemical measurements were carried out on a CHI660B electrochemical workstation with a conventional three-electrode cell. A platinum plate was used as the counter electrode, an SCE was employed as the reference electrode, and the as-prepared Ni/NF, NiFe/NF, and bare NF were used as the working electrode. 1 M KOH solution with and without 0.33 M urea was employed as the electrolytes during the electrocatalysis. The UOR, OER, and HER measurements were evaluated using linear sweep voltammetry (LSV) with a scan rate of 5 mV s^{-1} . The potentials were calibrated to a reversible hydrogen electrode (RHE) according to the equation: $E_{\text{RHE}} = E_{\text{SCE}} + 0.24 + 0.059 \text{ pH}$ where $\text{pH} = 14$, E_{SCE} is the measured potential versus SCE. The electrochemically active surface area (ESCA) of electrodes were calculated to evaluate the electrocatalytic properties by determining the electrochemical double-layer capacitance (Cdl) from the cyclic voltammetry (CV) curves.

3. RESULTS AND DISCUSSION

3.1. UOR and OER catalytic performance

The UOR catalytic performance of NF, Ni/NF, and NiFe/NF was first evaluated. Figure 1A shows the typical LSV curves of NF, Ni/NF, and NiFe/NF in 1 M KOH and 0.33 M urea at the potential scan rate of 5 mV s^{-1} . As can be seen from the figure, the bare NF shows inferior UOR activity, the onset potential is about 1.4 V. Both the Ni/NF and NiFe/NF exhibit superior UOR activity, and the onset potentials are 1.35 V and 1.3V. The anodic current steep rises with the potential to become more positive. It is obvious that the current density of NiFe/NF is higher than that of Ni/NF at 1.4 V (vs RHE), suggesting its more excellent UOR catalytic performance.



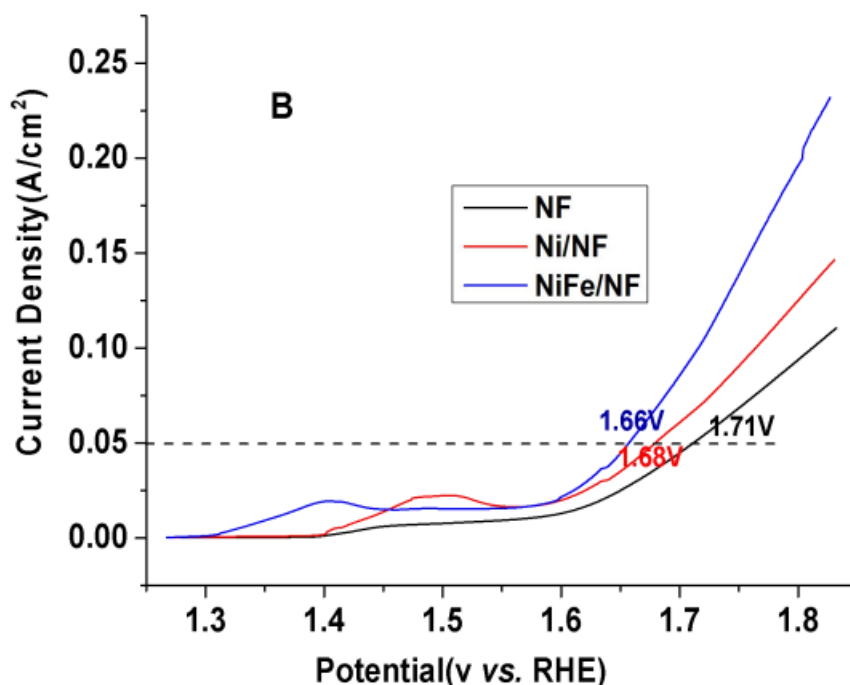


Figure 1. (A) LSV curves of NF, Ni/NF, and NiFe/NF in 1 M KOH and 0.33 M urea at the potential scan rate of 5 mV s^{-1} . (B) LSV curves of NF, Ni/NF, and NiFe/NF in 1 M KOH without urea.

A very low potential (1.36 V vs. RHE) was required affording the benchmark current density (50 mA cm^{-2}). However, the Ni/NF and NF require 1.39V and 1.44 V to achieve the same current density. The results exhibit the best UOR catalytic activity of NiFe/NF.

The OER catalytic performance of NF, Ni/NF, and NiFe/NF was also evaluated. The oxidation peak observed at 1.4 V is ascribed to one electron reaction of $\text{Ni}^{2+}/\text{Ni}^{3+}$. The OER catalytic activity was assessed by comparing the main parameter of the overpotential required[27]. Figure 1B shows the typical LSV curves of NF, Ni/NF, and NiFe/NF in 1 M KOH without urea at the potential scan rate of 5 mV s^{-1} . As can be seen in Figure 1B, affording the benchmark current density (50 mA cm^{-2}), potentials of 1.66 V, 1.68V, and 1.71V were required for NF, Ni/NF, and NiFe/NF. The above results indicate that NiFe/NF has superior OER catalytic performance than those of Ni/NF and NF. For NiFe/NF, the potentials of 1.36 and 1.66 V were required to afford 50 mA cm^{-2} for UOR and OER, respectively. The large gap(0.3V) in potential between UOR and OER suggesting that it is much easier to oxidize urea than water[28].

3.2. HER catalytic performance

The HER electrocatalytic performance of NF, Ni/NF, and NiFe/NF was evaluated by a typical three-electrode system at room temperature. Figure 2 shows the typical LSV curves of NF, Ni/NF, and NiFe/NF in 1.0M KOH and 0.33 M urea.

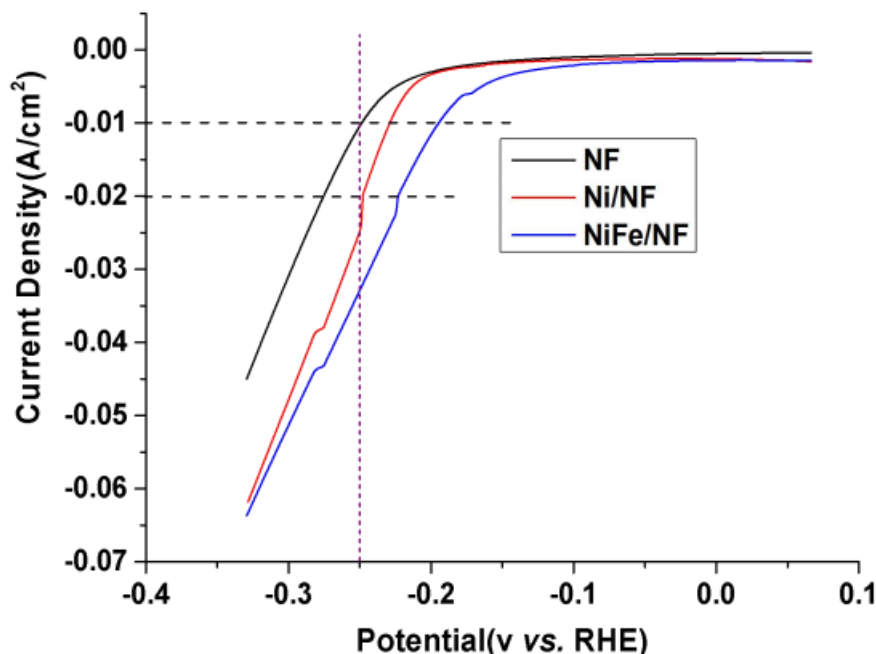
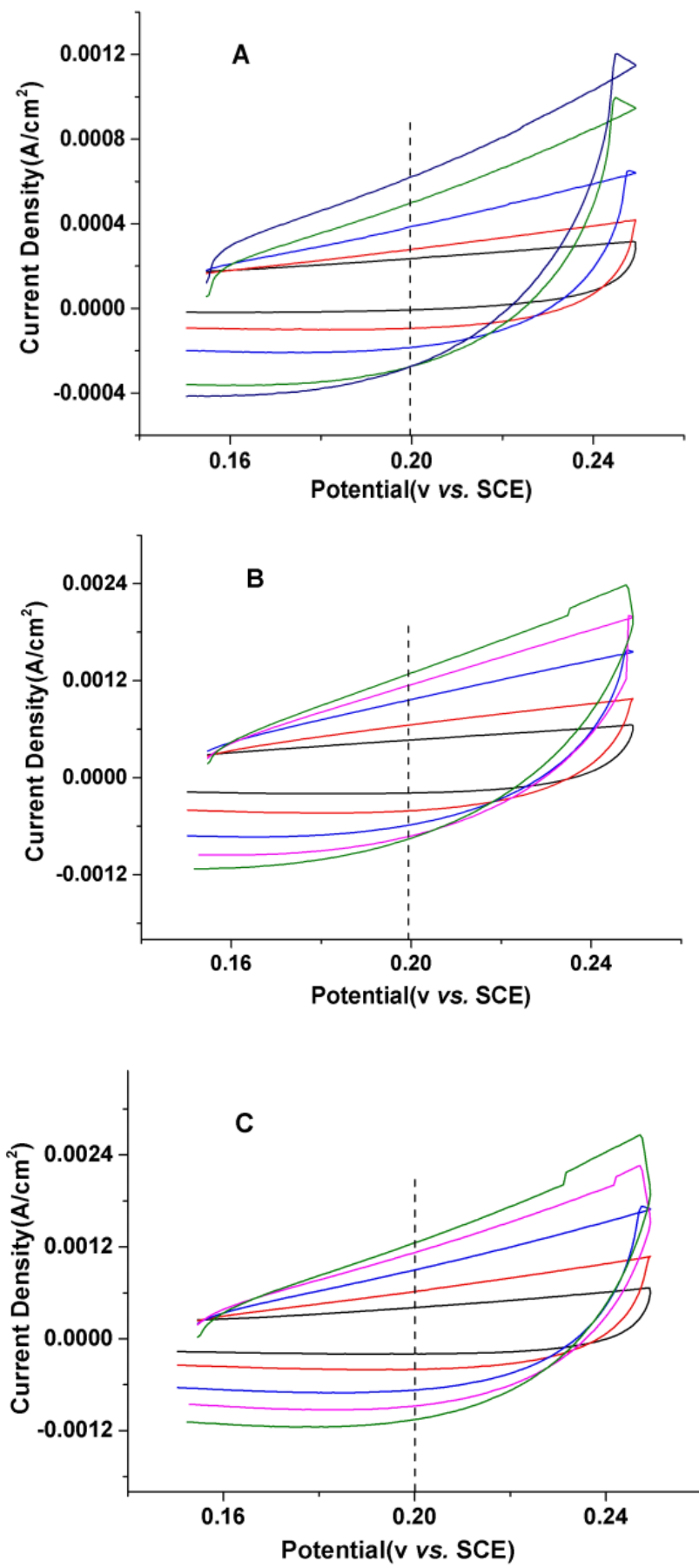


Figure 2. LSV curves of NF, Ni/NF, and NiFe/NF in 1.0M KOH and 0.33 M urea.

As can be seen, bare NF required a much higher overpotential to drive the same cathodic current (10 mA cm^{-2} or 20 mA cm^{-2}). Ni/NF and NiFe/NF exhibited high catalytic activity, indicating their successful HER catalysis application in the KOH solution. Obviously, the NiFe/NF delivered the smallest overpotential at the same current densities (10 mA cm^{-2} or 20 mA cm^{-2}). In other words, NiFe/NF delivered a higher current density at a given potential value (-0.25 V).

3.3. Electrochemically active surface area

Electrochemically active surface area (ESCA) was tested to elucidate the high UOR activity of NiFe/NF. ESCA is an effective parameter which is used to show the catalytic activity of a catalyst. Large ESCA normally suggests more active sites of a catalyst and improvement of the catalytic activity. The ESCA of electrodes were evaluated by using the electrochemical double-layer capacitance (Cdl) which was determined from the CV curves [29]. By plotting the current density versus scan rates, a linear slope can be obtained, which has a positive correlation with Cdl. Figure 3A-C shows the CV curves of NF, Ni/NF, and NiFe/NF in 1.0M KOH solution with different scan rates from 10 to 50 mV s^{-1} . The corresponding Cdl of the catalysts were shown in Figure 3D.



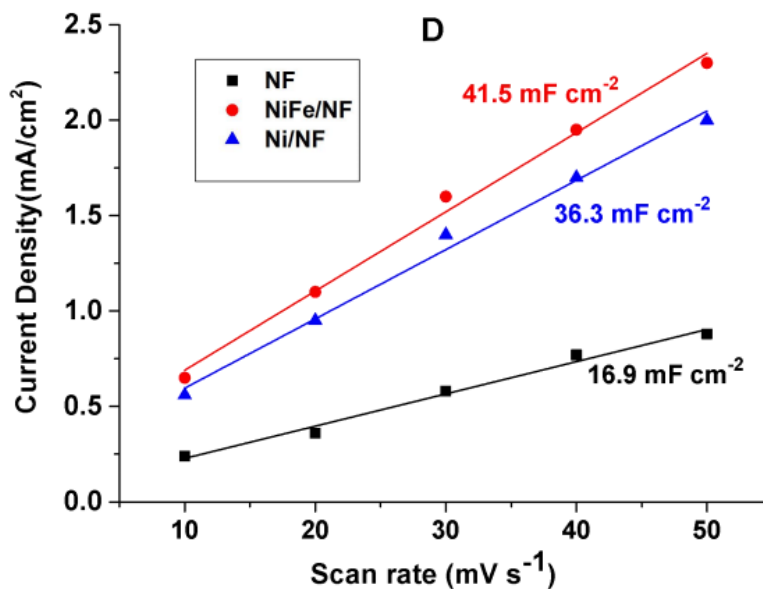


Figure 3. CV curves of (A) NF, (B) Ni/NF, and (C) NiFe/NF with different scan rates from 10 to 50 mV s⁻¹. (D) Plots of the corresponding current density against scan rate for NF, Ni/NF, and NiFe/NF.

As can be seen, the Cdl values of the NF, Ni/NF, and NiFe/NF were 16.9, 36.3, and 41.5 mF cm⁻², respectively. Thus, NiFe/NF has the highest Cdl value, indicating that NiFe/NF has an improved ESCA and more active sites than those of NF and Ni/NF.

4. CONCLUSION

In this work, the as-prepared NiFe/NF showed excellent electrocatalytic activities for HER and UOR in 1.0M KOH and 0.33 M urea. For UOR catalysis, a potential of 1.36 V vs. RHE was required affording the benchmark current density of 50 mA cm⁻² which was lower than those of Ni/NF and NF. At HER catalysis application in the KOH solution, the NiFe/NF delivered the smallest overpotential at the same current densities (10 mA cm⁻² or 20 mA cm⁻²). For ESCA measurements, NiFe/NF has the highest Cdl value, indicating that NiFe/NF has an improved ESCA and more active sites than those of NF and Ni/NF.

ACKNOWLEDGMENT

This work was sponsored by the National Natural Science Foundation of China (No.51077013, No.21506102), the Natural Science Foundation of Jiangsu Higher Education Institutions of China(No.18KJB150023), the Municipal Key Subjects of Environmental Science and Engineering, Nanjing Xiaozhuang University (No.4136001).

References

1. I. Dincer and C. Acar, *Int. J. Hydrogen Energ.*, 43(2018)8579.
2. Q. Sun, J. Liu, B. Xiao, B. Wang, M. Banis, H. Yadegari, K. R. Adair, R. Li and X. Sun, *Adv. Funct. Mater.*, 29(2019)1808332.

3. Y. Tong, P. Chen, M. Zhang, T. Zhou, L. Zhang, W. Chu, C. Wu and Y. Xie, *ACS Catalysis*, 8(2018)1.
4. C. Tang, R. Zhang, W. Lu, Z. Wang, D. Liu, S. Hao, G. Du, A. M. Asiri and X. Sun. *Angew. Chem.*, 129 (2017) 860.
5. B. Xia, Y. Yan, N. Li, H. Wu, X. Lou and X. Wang, *Nat. Energy*, 1(2016)15006.
6. J. Li and G. Zheng, *Adv. Sci.*, 4(2017)1600380.
7. D. Zhu, C. Guo, J. Liu, L. Wang, Y. Dub and S. Qiao, *Chem. Commun.*, 53 (2017) 10906.
8. Y. Li, H. Wang, R. Wang, B. He and Y. Gong, *Mater. Res. Bull.*, 100(2018)72.
9. X. Han, X. Wu, Y. Deng, J. Liu, J. Lu, C. Zhong and W. Hu, *Adv. Energ. Mater.*, 8 (2018)1870110.
10. P.S.M. Kumar, V.K. Ponnusamy, K.R. Deepthi, G. Kumar, A. Pugazhendhi, H. Abe, S. Thiripuranthagan, U. Pal and S.K. Krishnan, *J. Mater. Chem. A*, 6 (2018) 23435.
11. R. Prasannachandran, T.V. Vineesh, A. Anil, B.M. Krishna and M.M. Shaijumon, *ACS Nano*, 12 (2018) 11511.
12. L. Jiao, Y. Zhou and H. Jiang, *Chem. Sci.*, 7 (2016) 1690.
13. N. Senthilkumar, G. K. Gnana and A. Manthiram, *Adv. Energ. Mater.*, 8 (2018)1702207.
14. V. Prabhakaran, C.G. Arges and V. Ramani, *P. Natl. Acad. Sci.*, 109 (2012) 1029.
15. L. Wang, S. Zhu, N. Marinkovic, S. Kattel, M. Shao, B. Yang and J. Chen, *Appl. Catal. B- Environ.*, 232 (2018) 365.
16. R. Lan, S. Tao and J.T. Irvine, *Energ. Environ. Sci.*, 3 (2010) 438.
17. B.K. Boggs, R.L. King and G.G. Botte, *Chem. Commun.*, 32(2009) 4859.
18. J. Lim, A. Savchenkov, E. Dale, W. Liang, D. Eliyahu, V. Ilchenko, A. Matsko, L. Maleki and C. Wong, *Nat. Commun.*, 8 (2017) 8.
19. Y. Fu, H. Yu, C. Jiang, T. Zhang, R. Zhan, X. Li, J. Li, J. Tian and R. Yang, *Adv. Funct. Mater.*, 28 (2018) 1705094.
20. Z. Yu, C. Lang, M. Gao, Y. Chen, Q. Fu, Y. Duan and S. Yu. *Energ. Environ. Sci.*, 11 (2018) 1890.
21. J.W. Ng, M. García-Melchor, M. Bajdich, M. Bajdich, P. Chakthranont, C. Kirk, A. Vojvodic and T. Jaramillo, *Nat. Energy*, 1 (2016) 16053.
22. H. Xu, J. Wei, K. Zhang, Y. Shiraish and Y. Du, *ACS Appl. Mater. Inter.*, 10 (2018)29647.
23. Y. Jia, L. Zhang, G. Gao, H. Chen, B. Wang, J. Zhou, M. Soo, M. Hong, X. Yan and G. Qian, *Adv. Mater.*, 29 (2017) 1700017.
24. L. Yu, H. Zhou, J. Sun, F. Qin, F. Yu, J. Bao, Y. Yu, S. Chen and Z. Ren, *Energ. Environ. Sci.*, 10 (2017) 1820.
25. P. Jiang, Y. Yang, R. Shi, G. Xia, J. Chen, J. Su and Q. Chen, *J. Mater. Chem. A*, 5 (2017) 5475.
26. R.L. King and G.G. Bott, *J. Power Sources*, 196 (2011) 9579.
27. Z. Wang, P. Guo, M. Liu, C. Guo, H. Liu, S. Wei, J. Zhang and X. Lu, *ACS Appl. Energy Mater.*, 2 (2019)3363.
28. P. Babar, A. Lokhande, H. H. Shin, B. Pawar, M. G. Gang, S. Pawar and J. H. Kim, *Small*, 14 (2018)1702568.
29. P. Babar, A. C. Lokhande, B. S. Pawar, M. G. Gang, E. Jo, C. Go, M. P. Suryawanshi, S. M. Pawar, and J. H. Kim, *Appl. Surf. Sci.*, 427 (2018) 253–259.